

# Central exclusive production of axial-vector $f_1$ mesons in proton-proton collisions within the tensor-pomeron approach

Piotr Lebiedowicz\*

Institute of Nuclear Physics Polish Academy of Sciences,  
Radzikowskiego 152, PL-31342 Kraków, Poland

\* [Piotr.Lebiedowicz@ifj.edu.pl](mailto:Piotr.Lebiedowicz@ifj.edu.pl)

*Proceedings for the XXXIII International Workshop on High Energy Physics,  
Hard Problems of Hadron Physics: Non-Perturbative QCD & Related Quests  
ONLINE, 8-12 November 2021  
doi:10.21468/SciPostPhysProc.6*

## Abstract

We discuss the central exclusive production of  $f_1$  mesons in proton-proton collisions. The diffractive pomeron-pomeron fusion process within the tensor-pomeron approach is considered. Two ways to construct the pomeron-pomeron- $f_1$  coupling are discussed. The theoretical calculation of coupling constants is a challenging problem of nonperturbative QCD. We adjust the parameters of the model to the WA102 experimental data. The total cross section and differential distributions are presented. Predictions for LHC experiments are given. Detailed analysis of the distributions in  $\phi_{pp}$  the azimuthal angle between the transverse momenta of the outgoing protons can help to check different models and to study real pattern of the absorption effects.



Copyright P. Lebiedowicz *et al.*

This work is licensed under the Creative Commons

[Attribution 4.0 International License](https://creativecommons.org/licenses/by/4.0/).

Published by the SciPost Foundation.

Received 13-01-2022

Accepted 14-04-2022

Published 31-05-2022

doi:[10.21468/SciPostPhysProc.6.010](https://doi.org/10.21468/SciPostPhysProc.6.010)



Check for updates

## 1 Introduction

In this contribution we discuss central exclusive production (CEP) of axial-vector  $f_1$  ( $J^{PC} = 1^{++}$ ) mesons in proton-proton collisions

$$p(p_a, \lambda_a) + p(p_b, \lambda_b) \rightarrow p(p_1, \lambda_1) + f_1(k, \lambda) + p(p_2, \lambda_2), \quad (1)$$

where  $p_{a,b}$ ,  $p_{1,2}$  and  $\lambda_{a,b}$ ,  $\lambda_{1,2} = \pm 1/2$  denote the four-momenta and helicities of the protons, and  $k$  and  $\lambda = 0, \pm 1$  denote the four-momentum and helicity of the  $f_1$  meson, respectively. Here  $f_1$  stands for one of the axial-vector mesons with  $J^{PC} = 1^{++}$ , i.e.  $f_1(1285)$  or  $f_1(1420)$ . This presentation summarises some of the key results of [1] to which we refer the reader for further details. CEP of  $f_1(1285)$  and  $f_1(1420)$  mesons was measured by WA102 Collaboration [2–4]. Their internal structure ( $q\bar{q}$ , tetraquark,  $K\bar{K}$  molecule) remains to be established. At high energies the double-pomeron exchange mechanism (Figure 1) is expected to be dominant.

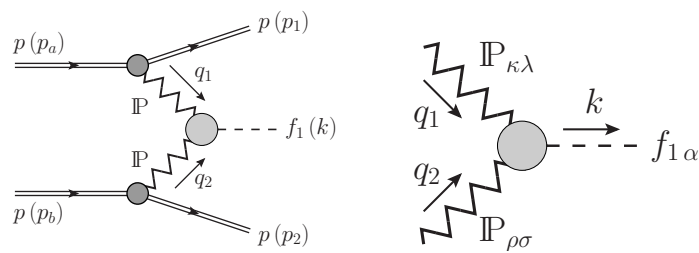


Figure 1: Diagrams for the reaction (1) with double- $\mathbb{P}$  exchange and the  $\mathbb{P}\mathbb{P}f_1$  vertex.

The pomeron ( $\mathbb{P}$ ) is essential object for understanding diffractive phenomena. Within QCD is a color singlet, predominantly gluonic object, thus the CEP of mesons has long been regarded as a potential source of glueballs.

For soft reactions, calculations of the pomeron from first principle are currently not possible, and one has to retreat to Regge models to describe soft high-energy diffractive scattering. Until recently, the spin structure of the pomeron has not received much attention. It is well known that the pomeron carries vacuum quantum numbers with regard to charge, color, isospin and charge conjugation. But what about spin? It has been shown some time ago that the charge-conjugation  $C = +1$  pomeron can be regarded as a coherent sum of elementary spin  $2 + 4 + 6 + \dots$  exchanges [5]. The tensor-pomeron model introduced in [6] assumes this property. We treat the reaction (1) in this model, in which the pomeron exchange is described as effective rank 2 symmetric tensor exchange. This approach has a good basis from nonperturbative QCD using functional integral techniques [5]. A tensor character of the pomeron is also preferred in holographic QCD models [7–10].

The tensor-pomeron model was applied to two-body hadronic reactions [6, 11, 12], to photoproduction of  $\pi^+\pi^-$  pairs [13], to low- $x$  deep inelastic lepton-nucleon scattering and photoproduction [14], and especially to CEP reactions

$$p + p \rightarrow p + X + p, \quad X = \eta, \eta', f_0, f_1, f_2, \pi^+\pi^-, K^+K^-, p\bar{p}, 4\pi, 4K, \rho^0, \phi, \phi\phi, K^{*0}\bar{K}^{*0}; \quad (2)$$

see e.g. [15–21]. In this model the  $C = -1$  odderon [22] is described as effective vector exchange. Exclusive reactions suitable for studies of the odderon exchange at high energies were discussed in [13, 19, 20]. Conceptually, vector-type couplings of the pomeron turn out to be rather questionable. For example, a vector pomeron implies that the total cross sections for  $pp$  and  $p\bar{p}$  scattering at high energy have opposite sign [11]. But, of course, quantum field theory forbids negative cross sections. A further argument against a vector pomeron was shown in [14], mainly it does not give any contribution to photoproduction data. One may also ask about the possibility of a scalar coupling of the pomeron to external particles. While possible from the point of view of QFT, such a coupling is experimentally disfavoured. In [11] it was shown that STAR data [23] on polarised elastic  $pp$  scattering are compatible with the tensor-pomeron ansatz but clearly rule out a scalar character of the soft pomeron what its coupling concerns. Also some historical remarks on different views of the pomeron were made in [11]. In the light of our discussion here we cannot support the conclusions of [24, 25] that the pomeron behaves (couples) like vector current.

The theoretical calculation of  $\mathbb{P}\mathbb{P}f_1$  coupling is a challenging problem of nonperturbative QCD. We argue that the pomeron couplings play an important role, and that they should be treated as tensor couplings. Using our model we perform a fit to the available WA102 data [2, 4] and we analyse whether our study could shed light on the  $\mathbb{P}\mathbb{P}f_1$  couplings. In the future the model parameters ( $\mathbb{P}\mathbb{P}f_1$  coupling constants, cutoff parameters in form factors) could be adjusted by comparison with precise experimental data from both RHIC and the LHC.

The  $\pi^+\pi^-\pi^+\pi^-$  channel seems well suited to measure the  $f_1(1285)$  CEP at high energies. For a preliminary data of the reaction  $pp \rightarrow pp2\pi^+2\pi^-$  measured at LHC@13TeV by the ATLAS Collaboration see [26].

## 2 Sketch of the formalism

### 2.1 The amplitude for the $pp \rightarrow ppf_1$ reaction

The Born-level amplitude for the reaction (1) via pomeron-pomeron fusion (Figure 1) can be written as

$$\begin{aligned} \mathcal{M}_{\lambda_a\lambda_b \rightarrow \lambda_1\lambda_2\lambda}^{\text{Born}} &= (-i)(\epsilon^\mu(\lambda))^* \bar{u}(p_1, \lambda_1) i\Gamma_{\mu_1\nu_1}^{(\mathbb{P}pp)}(p_1, p_a) u(p_a, \lambda_a) \\ &\quad \times i\Delta^{(\mathbb{P})\mu_1\nu_1, \alpha_1\beta_1}(s_1, t_1) i\Gamma_{\alpha_1\beta_1, \alpha_2\beta_2, \mu}^{(\mathbb{P}f_1)}(q_1, q_2) i\Delta^{(\mathbb{P})\alpha_2\beta_2, \mu_2\nu_2}(s_2, t_2) \\ &\quad \times \bar{u}(p_2, \lambda_2) i\Gamma_{\mu_2\nu_2}^{(\mathbb{P}pp)}(p_2, p_b) u(p_b, \lambda_b). \end{aligned} \quad (3)$$

The relevant kinematic quantities are

$$\begin{aligned} s &= (p_a + p_b)^2, \quad s_1 = (p_a + q_2)^2 = (p_1 + k)^2, \quad s_2 = (p_b + q_1)^2 = (p_2 + k)^2, \\ k &= q_1 + q_2, \quad q_1 = p_a - p_1, \quad q_2 = p_b - p_2, \quad t_1 = q_1^2, \quad t_2 = q_2^2, \quad m_{f_1}^2 = k^2. \end{aligned} \quad (4)$$

In (3)  $\epsilon^\mu(\lambda)$  is the polarisation vector of the  $f_1$  meson,  $\Delta^{(\mathbb{P})}$  and  $\Gamma^{(\mathbb{P}pp)}$  denote the effective propagator and proton vertex function, respectively, for the tensor-pomeron exchange [6]. The new quantity, to be studied here, is the  $\mathbb{P}f_1$  coupling (vertex function). In our analysis we should also include absorption effects to the Born amplitude. Then the full amplitude is

$$\mathcal{M}_{pp \rightarrow ppf_1} = \mathcal{M}_{pp \rightarrow ppf_1}^{\text{Born}} + \mathcal{M}_{pp \rightarrow ppf_1}^{\text{pp-rescattering}}. \quad (5)$$

The amplitude including the  $pp$ -rescattering corrections can be written as (within the one-channel-eikonal approach)

$$\mathcal{M}_{pp \rightarrow ppf_1}^{\text{pp-rescattering}}(s, \mathbf{p}_{t,1}, \mathbf{p}_{t,2}) = \frac{i}{8\pi^2 s} \int d^2\mathbf{k}_t \mathcal{M}_{pp \rightarrow ppf_1}^{\text{Born}}(s, \tilde{\mathbf{p}}_{t,1}, \tilde{\mathbf{p}}_{t,2}) \mathcal{M}_{pp \rightarrow pp}(s, t), \quad (6)$$

where  $\mathbf{p}_{t,1}$  and  $\mathbf{p}_{t,2}$  are the transverse components of the momenta of the outgoing protons and  $\mathbf{k}_t$  is the transverse momentum carried around the pomeron loop.  $\mathcal{M}_{pp \rightarrow ppf_1}^{\text{Born}}$  is the Born amplitude given by (3) with  $\tilde{\mathbf{p}}_{t,1} = \mathbf{p}_{t,1} - \mathbf{k}_t$  and  $\tilde{\mathbf{p}}_{t,2} = \mathbf{p}_{t,2} + \mathbf{k}_t$ .  $\mathcal{M}_{pp \rightarrow pp}$  is the elastic  $pp$  scattering amplitude for large  $s$  and with the momentum transfer  $t = -\mathbf{k}_t^2$ . In practice we work with the amplitudes in the high-energy approximation, i.e. assuming  $s$ -channel helicity conservation in the pomeron-proton vertex.

### 2.2 The pomeron-pomeron- $f_1$ coupling

We follow two strategies for constructing the  $\mathbb{P}f_1$  coupling and the vertex function.

(1) Phenomenological approach. First we consider a fictitious process: the fusion of two “real spin-2 pomerons” (or tensor glueballs) of mass  $m$  giving an  $f_1$  meson of  $J^{PC} = 1^{++}$ . We make an angular momentum analysis of this reaction in its c.m. system, the rest system of the  $f_1$  meson:  $\mathbb{P}(m, \epsilon_1) + \mathbb{P}(m, \epsilon_2) \rightarrow f_1(m_{f_1}, \epsilon)$ . The spin 2 of these “pomerons” can be combined to a total spin  $S$  ( $0 \leq S \leq 4$ ) and this must be combined with the orbital angular momentum  $l$  to give the  $J^{PC} = 1^{++}$  values of the  $f_1$ . There are two possibilities,  $(l, S) = (2, 2)$  and  $(4, 4)$

(see Appendix A of [15]), and corresponding coupling Lagrangians  $\mathbb{P}\mathbb{P}f_1$  are:

$$\mathcal{L}_{\mathbb{P}\mathbb{P}f_1}^{(2,2)} = \frac{g'_{\mathbb{P}\mathbb{P}f_1}}{32 M_0^2} \left( \mathbb{P}_{\kappa\lambda} \overleftrightarrow{\partial}_\mu \overleftrightarrow{\partial}_\nu \mathbb{P}_{\rho\sigma} \right) \left( \partial_\alpha U_\beta - \partial_\beta U_\alpha \right) \Gamma^{(8)\kappa\lambda,\rho\sigma,\mu\nu,\alpha\beta}, \quad (7)$$

$$\mathcal{L}_{\mathbb{P}\mathbb{P}f_1}^{(4,4)} = \frac{g''_{\mathbb{P}\mathbb{P}f_1}}{24 \cdot 32 \cdot M_0^4} \left( \mathbb{P}_{\kappa\lambda} \overleftrightarrow{\partial}_{\mu_1} \overleftrightarrow{\partial}_{\mu_2} \overleftrightarrow{\partial}_{\mu_3} \overleftrightarrow{\partial}_{\mu_4} \mathbb{P}_{\rho\sigma} \right) \left( \partial_\alpha U_\beta - \partial_\beta U_\alpha \right) \Gamma^{(10)\kappa\lambda,\rho\sigma,\mu_1\mu_2\mu_3\mu_4,\alpha\beta}, \quad (8)$$

where  $M_0 \equiv 1$  GeV (introduced for dimensional reasons),  $g'_{\mathbb{P}\mathbb{P}f_1}$  and  $g''_{\mathbb{P}\mathbb{P}f_1}$  are dimensionless coupling constants,  $\mathbb{P}_{\kappa\lambda}$  is the  $\mathbb{P}$  effective field,  $U_\alpha$  is the  $f_1$  field, and  $\Gamma^{(8)}$ ,  $\Gamma^{(10)}$  are known tensor functions [1].

(2) Our second approach uses holographic QCD, in particular the Sakai-Sugimoto model [27–29] where the  $\mathbb{P}\mathbb{P}f_1$  coupling is determined by the mixed axial-gravitational anomaly of QCD. In this approach (see Appendix B of [1])

$$\mathcal{L}^{\text{CS}} = \chi' U_\alpha \varepsilon^{\alpha\beta\gamma\delta} \mathbb{P}^\mu_\beta \partial_\delta \mathbb{P}_{\gamma\mu} + \chi'' U_\alpha \varepsilon^{\alpha\beta\gamma\delta} \left( \partial_\nu \mathbb{P}^\mu_\beta \right) \left( \partial_\delta \partial_\mu \mathbb{P}^\nu_\gamma - \partial_\delta \partial^\nu \mathbb{P}_{\gamma\mu} \right) \quad (9)$$

with  $\chi'$  a dimensionless constant and  $\chi''$  a constant of dimension  $\text{GeV}^{-2}$ . For the CEP reaction, we use the  $\mathbb{P}\mathbb{P}f_1$  vertex derived from (9) supplemented by suitable form factor (11).

For our fictitious reaction ( $\mathbb{P} + \mathbb{P} \rightarrow f_1$ ) there is strict equivalence  $\mathcal{L}^{\text{CS}} \equiv \mathcal{L}^{(2,2)} + \mathcal{L}^{(4,4)}$  if the couplings satisfy the relations

$$g'_{\mathbb{P}\mathbb{P}f_1} = -\chi' \frac{M_0^2}{k^2} - \chi'' \frac{M_0^2(k^2 - 2m^2)}{2k^2}, \quad g''_{\mathbb{P}\mathbb{P}f_1} = \chi'' \frac{2M_0^4}{k^2}. \quad (10)$$

For our CEP reaction (1) we are dealing with pomerons of mass squared  $t_1, t_2 < 0$  and, in general,  $t_1 \neq t_2$ . Then, the equivalence relation for small values  $|t_1|$  and  $|t_2|$  will still be approximately true and we confirm this by explicit numerical studies (see Fig. 11 of [1]).

For realistic applications we should multiply the “bare” vertex  $\Gamma^{(\mathbb{P}\mathbb{P}f_1)}(q_1, q_2)$  as derived from a corresponding coupling Lagrangian by a form factor  $\tilde{F}^{(\mathbb{P}\mathbb{P}f_1)}(t_1, t_2, k^2)$  which we take in the factorised ansatz

$$\tilde{F}^{(\mathbb{P}\mathbb{P}f_1)}(t_1, t_2, m_{f_1}^2) = \exp\left(\frac{t_1 + t_2}{\Lambda_E^2}\right), \quad (11)$$

where the cutoff constant  $\Lambda_E$  should be adjusted to experimental data.

As discussed in Appendix B of [1], the prediction for  $\chi''/\chi'$  obtained in the Sakai-Sugimoto model is

$$\chi''/\chi' = -(6.25 \cdots 2.44) \text{ GeV}^{-2} \quad (12)$$

for  $M_{\text{KK}} = (949 \cdots 1532)$  MeV. Usually [27]  $M_{\text{KK}}$  is fixed by matching the mass of the lowest vector meson to that of the physical  $\rho$  meson, leading to  $M_{\text{KK}} = 949$  MeV. However, this choice leads to a tensor glueball mass which is too low,  $M_T \approx 1.5$  GeV. The pomeron trajectory [ $\alpha_{\mathbb{P}}(t) = \alpha_{\mathbb{P}}(0) + \alpha'_{\mathbb{P}} t$ ,  $\alpha_{\mathbb{P}}(0) = 1.0808$ ,  $\alpha'_{\mathbb{P}} = 0.25 \text{ GeV}^{-2}$ ] corresponds to  $M_T \approx 1.9$  GeV, whereas lattice predictions correspond to  $M_T \gtrsim 2.4$  GeV.

## 3 Results

### 3.1 Comparison with the WA102 data

The WA102 collaboration obtained for the  $pp \rightarrow pp f_1(1285)$  reaction the total cross section of  $\sigma_{\text{exp}} = (6919 \pm 886)$  nb at  $\sqrt{s} = 29.1$  GeV and for a cut on the central system  $|x_F| \leq 0.2$  [2].

The WA102 collaboration also gave distributions in  $t$  and in  $\phi_{pp}$  ( $0 \leq \phi_{pp} \leq \pi$ ), the azimuthal angle between the transverse momenta of the two outgoing protons. We are assuming that the reaction (1) is dominated by pomeron exchange already at  $\sqrt{s} = 29.1$  GeV. In [4] an interesting behaviour of the  $\phi_{pp}$  distribution for  $f_1(1285)$  meson production for two different values of  $|t_1 - t_2|$  was presented. In Figure 2 we show some of our results [1] which include absorptive corrections; see Eqs. (5), (6). We show the  $\phi_{pp}$  distribution of events from [4] for  $|t_1 - t_2| \leq 0.2$  GeV<sup>2</sup> (left panels) and  $|t_1 - t_2| \geq 0.4$  GeV<sup>2</sup> (right panels). From the top panels, it seems that the  $(l, S) = (4, 4)$  term (8) best reproduces the shape of the WA102 data. The absorption effects play a significant role there. In the bottom panels of Fig. 2 we examine the combination of two  $\mathbb{P}\mathbb{P}f_1$  couplings  $\chi'$  and  $\chi''$  calculated with the vertex (9). The ratio (12) agrees with the fit  $\chi''/\chi' = -1.0$  GeV<sup>-2</sup> as far as the sign of this ratio is concerned, but not in its magnitude. This could indicate that the Sakai-Sugimoto model needs a more complicated form of reggeization of the tensor glueball propagator as indeed discussed in [29] in the context of CEP of  $\eta$  and  $\eta'$  mesons. It could also be an indication of the importance of secondary contributions with reggeon exchanges, i.e.  $\mathbb{R}\mathbb{R}$ -,  $\mathbb{R}\mathbb{P}$ -, and  $\mathbb{P}\mathbb{R}$ -fusion processes.

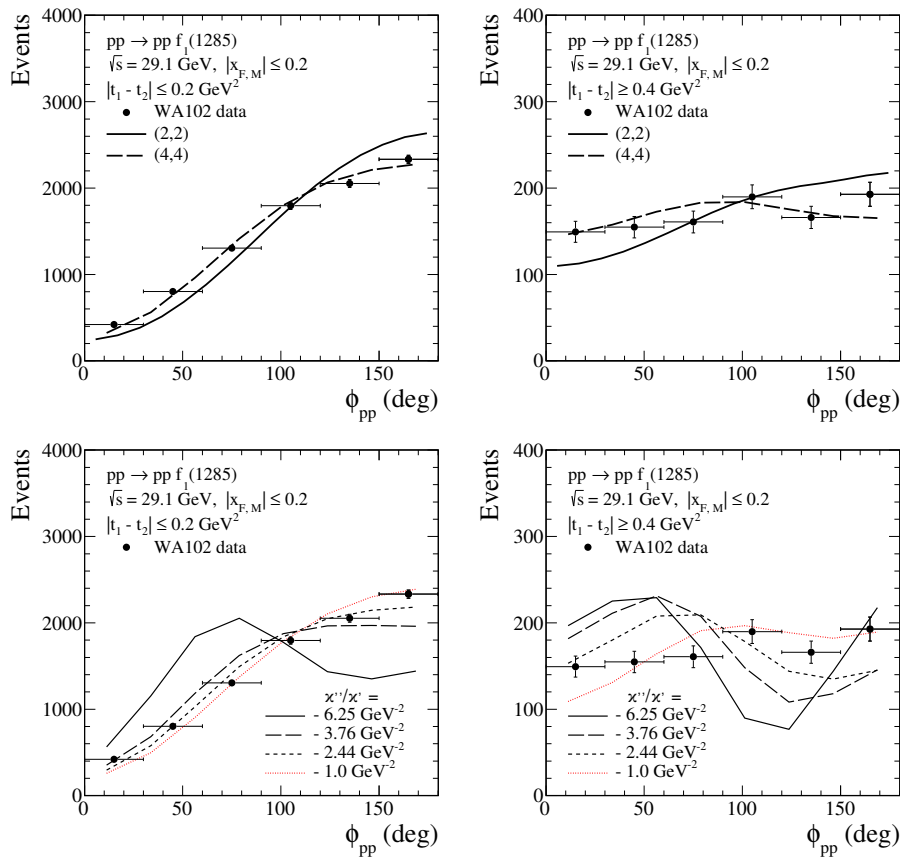


Figure 2: The  $\phi_{pp}$  distributions for  $f_1(1285)$  meson production at  $\sqrt{s} = 29.1$  GeV,  $|x_{F,M}| \leq 0.2$ , and for  $|t_1 - t_2| \leq 0.2$  GeV<sup>2</sup> (left panels) and  $|t_1 - t_2| \geq 0.4$  GeV<sup>2</sup> (right panels). The WA102 experimental data points are from Fig. 3 of [4]. The theoretical results have been normalised to the mean value of the number of events. The results for  $\Lambda_E = 0.7$  GeV a form-factor parameter (11) are shown.

We get a reasonable description of the WA102 data with  $\Lambda_E = 0.7$  GeV and the following

possibilities:

$$(l, S) = (2, 2) \text{ term only : } g'_{\mathbb{P}\mathbb{P}f_1} = 4.89, g''_{\mathbb{P}\mathbb{P}f_1} = 0; \quad (13)$$

$$(l, S) = (4, 4) \text{ term only : } g'_{\mathbb{P}\mathbb{P}f_1} = 0, g''_{\mathbb{P}\mathbb{P}f_1} = 10.31; \quad (14)$$

$$\text{CS terms : } \chi' = -8.88, \chi''/\chi' = -1.0 \text{ GeV}^{-2}. \quad (15)$$

Now we can use our equivalence relation (10) in order to see to which  $(l, S)$  couplings (15) corresponds. Replacing in (10)  $m^2$  by  $t_1 = t_2 = -0.1 \text{ GeV}^2$  and  $k^2$  by  $m_{f_1}^2 = (1282 \text{ MeV})^2$  we get from (15)

$$g'_{\mathbb{P}\mathbb{P}f_1} = 0.42, g''_{\mathbb{P}\mathbb{P}f_1} = 10.81. \quad (16)$$

Thus, the CS couplings of (15) correspond to a nearly pure  $(l, S) = (4, 4)$  coupling (14).

In Figure 3 we show the results for the  $\phi_{pp}$  distributions for different cuts on  $|t_1 - t_2|$  without and with the absorption effects included in the calculations. The results for the two  $(l, S)$  couplings are shown. The absorption effects lead to a large reduction of the cross section. We obtain the ratio of full and Born cross sections, the survival factor, as  $\langle S^2 \rangle = 0.5-0.7$ . Note that  $\langle S^2 \rangle$  depends on the kinematics. We can see a large damping of the cross section in the region of  $\phi_{pp} \sim \pi$ , especially for  $|t_1 - t_2| \geq 0.4 \text{ GeV}^2$ . We notice that our results for the  $(4, 4)$  term have similar shapes as those presented in [30] [see Figs. 3(c) and 3(d)] where the authors also included the absorption corrections.

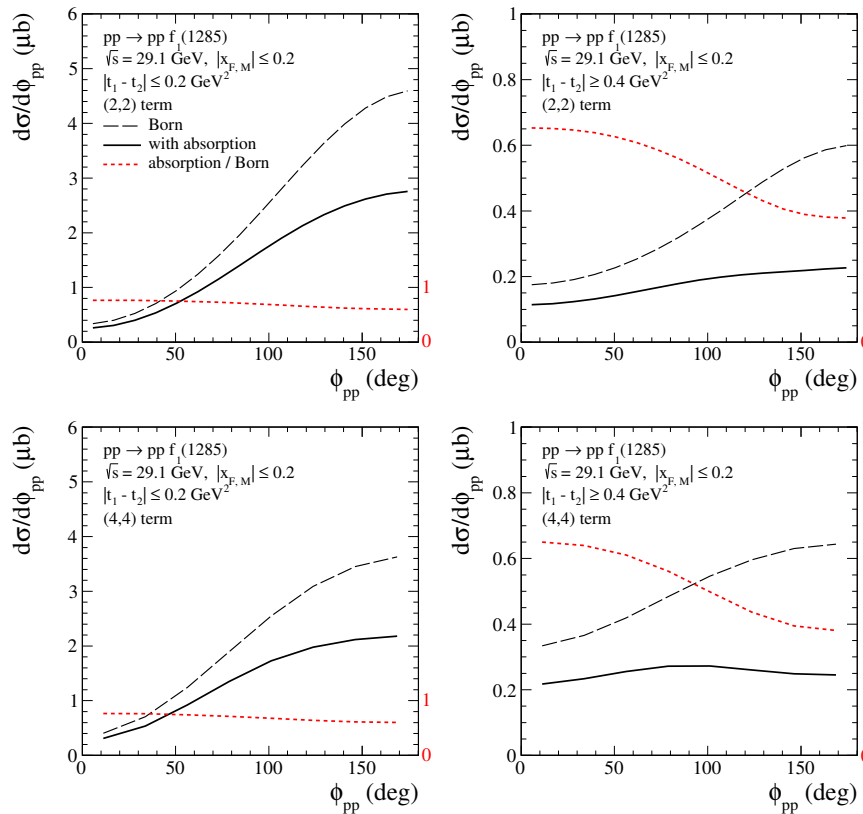


Figure 3: The  $\phi_{pp}$  distributions for  $f_1(1285)$  meson production at  $\sqrt{s} = 29.1 \text{ GeV}$ ,  $|x_{F,M}| \leq 0.2$ , for  $|t_1 - t_2| \leq 0.2 \text{ GeV}^2$  (left) and for  $|t_1 - t_2| \geq 0.4 \text{ GeV}^2$  (right). The long-dashed black lines represent the Born results and the solid black lines correspond to the results with the absorption effects included. The dotted red lines represent the ratio of full and Born cross sections on the scale indicated by the red numbers on the r.h.s. of the panels.

Having fixed the parameters of the model in this way we will give predictions for the LHC experiments. Because of the possible influence of nonleading exchanges at low energies, these predictions for cross sections at high energies should be regarded rather as an upper limit. The secondary reggeon exchanges should give small contributions at high energies and in the midrapidity region. As discussed in Appendix D of [1] we expect that they should overestimate the cross sections by not more than a factor of 4.

### 3.2 Predictions for the LHC experiments

Now we wish to show (selected) results for the  $pp \rightarrow pp f_1(1285)$  reaction for the LHC; see [1] for many more results. In Figure 4 we show our predictions for the distributions of  $\phi_{pp}$  and the transverse momentum of the  $f_1(1285)$  for  $\sqrt{s} = 13$  TeV,  $|y_M| < 2.5$ , and for the cut on the leading protons of  $0.17 \text{ GeV} < |p_{y,p}| < 0.50 \text{ GeV}$ . The results for the  $(l, S) = (2, 2)$  term (7), the  $(4, 4)$  term (8), and for the  $\chi'$  plus  $\chi''$  terms calculated with (9) for (12) obtained in the Sakai-Sugimoto model (see Appendix B of [1]) are shown. For comparison, the results for our fit to WA102 data ( $\chi''/\chi' = -1.0 \text{ GeV}^{-2}$ ) are also presented. The contribution with  $\chi''/\chi' = -6.25 \text{ GeV}^{-2}$  gives a significantly different shape. This could be tested in experiments, such as ATLAS-ALFA [26], when both protons are measured. We obtain the ratio of full and Born cross sections as  $\langle S^2 \rangle \simeq 0.3$  for  $\sqrt{s} = 13$  TeV.

The four-pion decay channel seems well suited to measure the CEP of the  $f_1(1285)$  at the LHC [26]. We predict a large cross section for the exclusive axial-vector  $f_1(1285) \rightarrow 4\pi$  production compared to the CEP of the tensor  $f_2(1270) \rightarrow 4\pi$  [16, 18]. The  $4\pi$  continuum for the  $pp \rightarrow pp4\pi$  reaction was studied in [17, 31].

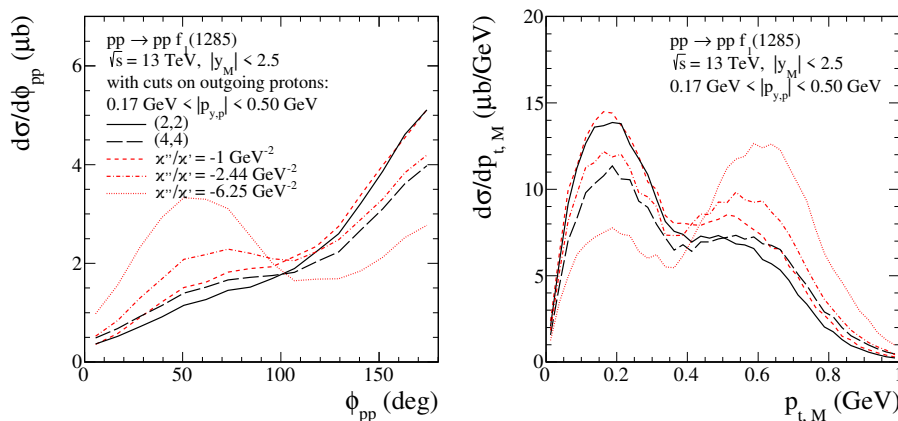


Figure 4: The differential cross sections for the  $f_1(1285)$  production at  $\sqrt{s} = 13$  TeV,  $|y_M| < 2.5$ , and with cuts on momenta of outgoing protons ( $0.17 \text{ GeV} < |p_{y,p}| < 0.50 \text{ GeV}$ ). The results for  $(l, S)$  and  $(\chi', \chi'')$  terms are shown.

## 4 Conclusion

- The calculations for the  $pp \rightarrow pp f_1(1285)$  reaction have been performed in the tensor-pomeron approach [6]. We have discussed in detail the forms of the  $\mathbb{P}\mathbb{P}f_1$  coupling. Detailed tests of the Sakai-Sugimoto model are possible.
- We obtain a good description of the WA102 data at  $\sqrt{s} = 29.1 \text{ GeV}$  [2, 4] assuming that the  $pp \rightarrow pp f_1(1285)$  reaction is dominated by pomeron-pomeron fusion.

- We obtain a large cross section for CEP of the  $f_1(1285)$  of  $\sigma \cong 6 - 40 \mu\text{b}$  for the ALICE, ATLAS-ALFA, CMS, and LHCb experiments, depending on the assumed cuts (see Table III of [1]). Predictions for the STAR experiments at RHIC are also given in [1]. In all cases the absorption effects were included.
- Experimental studies of single meson CEP reactions will allow to extract many PPM coupling parameters. The holographic methods applied to QCD already give some predictions [1, 29].
- Detailed analysis of the distributions in  $\phi_{pp}$ , the azimuthal angle between the transverse momenta of the outgoing protons, can help to solve several important problems for soft processes, to check/study the real pattern of the interaction (absorption models), to understand the difference in the dynamics of production of  $q\bar{q}$  mesons and glueballs (or more accurately, states which are believed to have a large glueball component), to disentangle  $f_1$ - and  $\eta$ -type resonances contributing to the same final channel.
- Such studies could be extended, for instance by the COMPASS experiment where presumably one could study the influence of reggeon-pomeron and reggeon-reggeon fusion terms. Future experiments available at the GSI-FAIR with HADES and PANDA should provide new information about the  $\rho\rho f_1$  and  $\omega\omega f_1$  couplings [32].

## Acknowledgements

The author is indebted to A. Szczurek, O. Nachtmann, A. Rebhan, and J. Leutgeb for their cooperation on this topic. Many thanks to R. Ryutin and V. Petrov for inviting me to the XXXIII International (ONLINE) Workshop on High Energy Physics and for useful discussions.

## References

- [1] P. Lebiedowicz, J. Leutgeb, O. Nachtmann, A. Rebhan and A. Szczurek, *Central exclusive diffractive production of axial-vector  $f_1(1285)$  and  $f_1(1420)$  mesons in proton-proton collisions*, Phys. Rev. D **102**, 114003 (2020), doi:[10.1103/PhysRevD.102.114003](https://doi.org/10.1103/PhysRevD.102.114003).
- [2] D. Barberis et al., *A measurement of the branching fractions of the  $f_1(1285)$  and  $f_1(1420)$  produced in central  $pp$  interactions at 450 GeV/c*, Phys. Lett. B **440**, 225 (1998), doi:[10.1016/S0370-2693\(98\)01264-7](https://doi.org/10.1016/S0370-2693(98)01264-7).
- [3] D. Barberis et al., *A spin analysis of the  $4\pi$  channels produced in central  $pp$  interactions at 450 GeV/c*, Phys. Lett. B **471**, 440 (2000), doi:[10.1016/S0370-2693\(99\)01413-6](https://doi.org/10.1016/S0370-2693(99)01413-6).
- [4] A. Kirk, *New effects observed in central production by experiment WA102 at the CERN Omega Spectrometer*, Nucl. Phys. A **663-664**, 608c (2000), doi:[10.1016/S0375-9474\(99\)00666-1](https://doi.org/10.1016/S0375-9474(99)00666-1).
- [5] O. Nachtmann, *Considerations concerning diffraction scattering in quantum chromodynamics*, Ann. Phys. **209**, 436 (1991), doi:[10.1016/0003-4916\(91\)90036-8](https://doi.org/10.1016/0003-4916(91)90036-8).
- [6] C. Ewerz, M. Maniatis and O. Nachtmann, *A model for soft high-energy scattering: Tensor pomeron and vector odderon*, Ann. Phys. **342**, 31 (2014), doi:[10.1016/j.aop.2013.12.001](https://doi.org/10.1016/j.aop.2013.12.001).

- [7] R. C. Brower, J. Polchinski, M. J. Strassler and C.-I. Tan, *The Pomeron and gauge/string duality*, J. High Energy Phys. **12**, 005 (2007), doi:[10.1088/1126-6708/2007/12/005](https://doi.org/10.1088/1126-6708/2007/12/005).
- [8] S. K. Domokos, J. A. Harvey and N. Mann, *The Pomeron contribution to  $pp$  and  $p\bar{p}$  scattering in AdS/QCD*, Phys. Rev. D **80**, 126015 (2009), doi:[10.1103/PhysRevD.80.126015](https://doi.org/10.1103/PhysRevD.80.126015).
- [9] A. Ballon-Bayona, R. Carcassés Quevedo, M. S. Costa and M. Djurić, *Soft Pomeron in holographic QCD*, Phys. Rev. D **93**, 035005 (2016), doi:[10.1103/PhysRevD.93.035005](https://doi.org/10.1103/PhysRevD.93.035005).
- [10] I. Iatrakis, A. Ramamurti and E. Shuryak, *Pomeron interactions from the Einstein-Hilbert action*, Phys. Rev. D **94**, 045005 (2016), doi:[10.1103/PhysRevD.94.045005](https://doi.org/10.1103/PhysRevD.94.045005).
- [11] C. Ewerz, P. Lebiedowicz, O. Nachtmann and A. Szczurek, *Helicity in proton-proton elastic scattering and the spin structure of the pomeron*, Phys. Lett. B **763**, 382 (2016), doi:[10.1016/j.physletb.2016.10.064](https://doi.org/10.1016/j.physletb.2016.10.064).
- [12] P. Lebiedowicz, O. Nachtmann and A. Szczurek, *High-energy  $\pi\pi$  scattering without and with photon radiation*, Phys. Rev. D **105**, 014022 (2022), doi:[10.1103/PhysRevD.105.014022](https://doi.org/10.1103/PhysRevD.105.014022).
- [13] A. Bolz, C. Ewerz, M. Maniatis, O. Nachtmann, M. Sauter and A. Schöning, *Photoproduction of  $\pi^+\pi^-$  pairs in a model with tensor-pomeron and vector-odderon exchange*, J. High Energy Phys. **01**, 151 (2015), doi:[10.1007/JHEP01\(2015\)151](https://doi.org/10.1007/JHEP01(2015)151).
- [14] D. Britzger, C. Ewerz, S. Glazov, O. Nachtmann and S. Schmitt, *The Tensor Pomeron and Low-x Deep Inelastic Scattering*, Phys. Rev. D **100**, 114007 (2019), doi:[10.1103/PhysRevD.100.114007](https://doi.org/10.1103/PhysRevD.100.114007).
- [15] P. Lebiedowicz, O. Nachtmann and A. Szczurek, *Exclusive central diffractive production of scalar and pseudoscalar mesons; tensorial vs. vectorial pomeron*, Ann. Phys. **344**, 301 (2014), doi:[10.1016/j.aop.2014.02.021](https://doi.org/10.1016/j.aop.2014.02.021).
- [16] P. Lebiedowicz, O. Nachtmann and A. Szczurek, *Central exclusive diffractive production of the  $\pi^+\pi^-$  continuum, scalar, and tensor resonances in  $pp$  and  $p\bar{p}$  scattering within the tensor Pomeron approach*, Phys. Rev. D **93**, 054015 (2016), doi:[10.1103/PhysRevD.93.054015](https://doi.org/10.1103/PhysRevD.93.054015).
- [17] P. Lebiedowicz, O. Nachtmann and A. Szczurek, *Exclusive diffractive production of  $\pi^+\pi^-\pi^+\pi^-$  via the intermediate  $\sigma\sigma$  and  $\rho\rho$  states in proton-proton collisions within tensor pomeron approach*, Phys. Rev. D **94**, 034017 (2016), doi:[10.1103/PhysRevD.94.034017](https://doi.org/10.1103/PhysRevD.94.034017).
- [18] P. Lebiedowicz, O. Nachtmann and A. Szczurek, *Extracting the Pomeron-Pomeron- $f_2(1270)$  coupling in the  $pp \rightarrow pp\pi^+\pi^-$  reaction through the angular distribution of the pions*, Phys. Rev. D **101**, 034008 (2020), doi:[10.1103/PhysRevD.101.034008](https://doi.org/10.1103/PhysRevD.101.034008).
- [19] P. Lebiedowicz, O. Nachtmann and A. Szczurek, *Searching for the odderon in  $pp \rightarrow ppK^+K^-$  and  $pp \rightarrow pp\mu^+\mu^-$  reactions in the  $\phi(1020)$  resonance region at the LHC*, Phys. Rev. D **101**, 094012 (2020), doi:[10.1103/PhysRevD.101.094012](https://doi.org/10.1103/PhysRevD.101.094012).
- [20] P. Lebiedowicz, O. Nachtmann and A. Szczurek, *Central exclusive diffractive production of  $K^+K^-K^+K^-$  via the intermediate  $\phi\phi$  state in proton-proton collisions*, Phys. Rev. D **99**, 094034 (2019), doi:[10.1103/PhysRevD.99.094034](https://doi.org/10.1103/PhysRevD.99.094034).
- [21] P. Lebiedowicz, *Study of the exclusive reaction  $pp \rightarrow ppK^{*0}\bar{K}^{*0}$ :  $f_2(1950)$  resonance versus diffractive continuum*, Phys. Rev. D **103**, 054039 (2021), doi:[10.1103/PhysRevD.103.054039](https://doi.org/10.1103/PhysRevD.103.054039).

- [22] V. M. Abazov et al., *Odderon Exchange from Elastic Scattering Differences between  $pp$  and  $p\bar{p}$  Data at 1.96 TeV and from  $pp$  Forward Scattering Measurements*, Phys. Rev. Lett. **127**, 062003 (2021), doi:[10.1103/PhysRevLett.127.062003](https://doi.org/10.1103/PhysRevLett.127.062003).
- [23] L. Adamczyk et al., *Single spin asymmetry  $A_N$  in polarized proton-proton elastic scattering at  $\sqrt{s} = 200$  GeV*, Phys. Lett. B **719**, 62 (2013), doi:[10.1016/j.physletb.2013.01.014](https://doi.org/10.1016/j.physletb.2013.01.014).
- [24] F. E. Close and G. A. Schuler, *Central production of mesons: Exotic states versus Pomeron structure*, Phys. Lett. B **458**, 127 (1999), doi:[10.1016/S0370-2693\(99\)00450-5](https://doi.org/10.1016/S0370-2693(99)00450-5).
- [25] F. E. Close and G. A. Schuler, *Evidence that the Pomeron transforms as a non-conserved vector current*, Phys. Lett. B **464**, 279 (1999), doi:[10.1016/S0370-2693\(99\)00875-8](https://doi.org/10.1016/S0370-2693(99)00875-8).
- [26] R. Sikora, *Measurement of the diffractive central exclusive production in the STAR experiment at RHIC and the ATLAS experiment at LHC*, Ph.D. thesis, AGH University of Science and Technology, Cracow, Poland, CERN-THESIS-2020-235 (2020).
- [27] T. Sakai and S. Sugimoto, *Low Energy Hadron Physics in Holographic QCD*, Prog. Theor. Phys. **113**, 843 (2005), doi:[10.1143/PTP113.843](https://doi.org/10.1143/PTP113.843).
- [28] F. Brünner, D. Parganlija and A. Rebhan, *Glueball decay rates in the Witten-Sakai-Sugimoto model*, Phys. Rev. D **91**, 106002 (2015), doi:[10.1103/PhysRevD.91.106002](https://doi.org/10.1103/PhysRevD.91.106002).
- [29] N. Anderson, S. K. Domokos, J. A. Harvey and N. Mann, *Central production of  $\eta$  and  $\eta'$  via double Pomeron exchange in the Sakai-Sugimoto model*, Phys. Rev. D **90**, 086010 (2014), doi:[10.1103/PhysRevD.90.086010](https://doi.org/10.1103/PhysRevD.90.086010).
- [30] V. Alexeevich Petrov, R. Anatolievich Ryutin, A. E. Sobol and J.-P. Guillaud, *Azimuthal angular distributions in EDDE as a spin-parity analyser and glueball filter for the LHC.*, J. High Energy Phys. **06**, 007 (2005), doi:[10.1088/1126-6708/2005/06/007](https://doi.org/10.1088/1126-6708/2005/06/007).
- [31] R. Kycia, P. Lebiedowicz, A. Szczurek and J. Turnau, *Triple Regge exchange mechanisms of four-pion continuum production in the  $pp \rightarrow pp\pi^+\pi^-\pi^+\pi^-$  reaction*, Phys. Rev. D **95**, 094020 (2017), doi:[10.1103/PhysRevD.95.094020](https://doi.org/10.1103/PhysRevD.95.094020).
- [32] P. Lebiedowicz, O. Nachtmann, P. Salabura and A. Szczurek, *Exclusive  $f_1(1285)$  meson production for energy ranges available at the GSI-FAIR with HADES and PANDA*, Phys. Rev. D **104**, 034031 (2021), doi:[10.1103/PhysRevD.104.034031](https://doi.org/10.1103/PhysRevD.104.034031).